Research Article

Cardioprotective Effects of Cephalandra indica Naud.-Mediated Gold Nanoparticles Against Stress-Induced Cardiomyopathy

Smita Jain*[1], Manju Prajapati[2]

School of Pharmacy, LNCT University, Bhopal, Madhya Pradesh, India 462042 Corresponding author: Smita Jain, Research Scholar, E-mail: jainsmita09@gmail.com

Abstract

Stress-induced cardiomyopathy is an acute cardiac condition associated with transient myocardial dysfunction and disturbances in redox homeostasis. The present study investigated the green synthesis of gold nanoparticles (AuNPs) using a methanolic leaf extract of Cephalandra indica and evaluated their protective activity in a rat model of stress-induced myocardial injury. Leaves were extracted with methanol by Soxhlet extraction, and the extract was subjected to preliminary phytochemical screening. AuNPs were synthesized using chloroauric acid and characterized by UV–visible spectroscopy, Fourier-transform infrared spectroscopy, X-ray diffraction, scanning electron microscopy, transmission electron microscopy, atomic force microscopy, energy-dispersive X-ray spectroscopy, and zeta-potential analysis. The methanolic extract yielded 15.24% w/w and showed alkaloids, flavonoids, phenolic compounds, tannins, terpenoids, saponins, and steroids. Nanoparticle formation was indicated by a ruby-red colour and a surface plasmon resonance band at 525 nm. SEM measurements in the supplied micrograph ranged from 31.52 to 46.65 nm, whereas TEM showed a mean particle diameter of 39.8 ± 0.8 nm. XRD reflections at approximately 38.14°, 44.76°, 64.80°, and 77.62° corresponded to the (111), (200), (220), and (311) planes of face-centred cubic gold. The zeta potential was −38.6 mV. In vivo, AuNP treatment shifted antioxidant parameters toward normal values and reduced LDH and TBARS compared with the stress-induced control. Histopathological examination also indicated improved preservation of myocardial architecture. These findings support further preclinical evaluation of C. indica-mediated AuNPs for stress-associated myocardial injury; mechanistic, pharmacokinetic, toxicological, and dose-optimization studies remain necessary before clinical translation.

Keywords: cardio protection; Cephalandra indica; gold nanoparticles; green synthesis; oxidative stress; stress-induced cardiomyopathy

1. Introduction

Psychological and emotional stress can adversely affect cardiovascular function through sustained activation of neuroendocrine and sympathetic pathways. Excess catecholamine release, oxidative imbalance, inflammatory signaling, endothelial dysfunction, altered calcium handling, and mitochondrial disturbances have been implicated in stress-associated myocardial injury (Cohen et al., 2007; Steptoe and Kivimäki 2012). Stress cardiomyopathy, also termed Takotsubo syndrome, is characterized by transient left ventricular dysfunction and may clinically resemble acute coronary syndromes.

Current understanding indicates that catecholamine excess and associated vascular, metabolic, inflammatory, and mitochondrial changes contribute to reversible myocardial stunning (Ghadri et al., 2018; Pelliccia et al., 2017). Supportive treatment may include beta-blockers, angiotensin-converting enzyme inhibitors or angiotensin receptor blockers, diuretics, and anticoagulants when clinically indicated. These approaches do not eliminate the need for investigation of complementary strategies that may modulate several components of stress-related myocardial injury (Brotman et al., 2007).

Medicinal plants provide chemically diverse secondary metabolites with antioxidant and anti-inflammatory properties. Cephalandra indica Naud. (syn. Coccinia grandis (L.) Voigt; ivy gourd) contains several phytochemical classes, including phenolics, flavonoids, alkaloids, terpenoids, glycosides, tannins, and saponins. Experimental literature has associated C. grandis with antioxidant, metabolic, and cytoprotective activities, while recent metabolomic profiling has identified numerous phenolic compounds, flavonoids, hydroxycinnamic acids, coumarins, lignans, and triterpenes, with leaves showing particularly high levels of flavonoids and hydroxycinnamic acids (Meenatchi et al. 2017; Lee et al., 2025).

Nevertheless, direct evidence for the activity of C. indica in stress-induced cardiomyopathy remains limited. Plant-derived constituents can also be constrained by solubility, chemical stability, metabolism, and bioavailability, creating a rationale for delivery approaches that may improve their physicochemical and biological performance (Fatima et al., 2024).

Gold nanoparticles have attracted biomedical interest because of their physicochemical stability, surface properties, functionalization potential, and applications in drug delivery and bioengineering. Green synthesis using plant extracts is particularly attractive because phytochemicals can participate in the reduction of gold ions and stabilization of the resulting nanoparticles (Iravani 2011; Mehra et al., 2024). Such phytochemical-associated surface chemistry may influence nanoparticle stability and biological interactions. Although C. indica has been investigated for antioxidant and metabolic effects and plant-mediated AuNPs have seen explored for biomedical applications, the combination of C. indica phytochemicals with AuNPs for stress-induced myocardial injury has not been adequately characterized. Therefore, the present study was designed to synthesize C. indica-mediated AuNPs, characterize their physicochemical properties, and examine their protective effects in an experimental model of stress-induced myocardial injury.

2. Materials and Methods

Plant material and authentication

Fresh leaves of Cephalandra indica were collected from the local area of Bhopal, Madhya Pradesh, India, in August 2025. The plant material was authenticated by Dr. Suman Mishra, MFP-PARC Vindhya Herbals, Bhopal, Madhya Pradesh, India. A voucher specimen (No. 181/Bot/MFP-PARC/2025) was deposited in the herbarium of the Botany Department.

2.1. Extraction

The leaves were shade-dried, coarsely powdered, and exhaustively extracted with methanol in a Soxhlet apparatus. The extract was filtered and concentrated under reduced pressure at a temperature below 45 °C. The reported extraction yield was 15.24%. The concentrated extract was further dried in a vacuum desiccator and stored in an airtight container until use (Harborne 1998).

2.2. Preliminary phytochemical screening

The methanolic extract was qualitatively screened for carbohydrates, glycosides, alkaloids, tannins, flavonoids, terpenoids, steroids, and saponins using standard pharmacognostic procedures (Kokate 2008).

Chemicals and reagents

Analytical-grade solvents, chemicals, and drugs were obtained from Hamidia Laboratories and Loba Chemie, Mumbai, India. Chloroauric acid ($HAuCl_4 \cdot 3H_2O$) was obtained from Sigma-Aldrich, St. Louis, MO, USA. Double-distilled water was used throughout the experimental procedures.

2.3. Green synthesis of AuNPs

Chloroauric acid (0.5 mM) was mixed with methanolic leaf extract (40 mg/mL), and the reaction mixture was maintained at 70 °C for 10 min. A change in colour from yellow to ruby red was used as an initial indication of nanoparticle formation. The reaction mixture was centrifuged at 12,000 rpm for 20 min, and the recovered nanoparticles were dried and stored as a powder for characterization and biological evaluation (Iravani 2011).

Characterization

The synthesized AuNPs were characterized using UV–visible spectroscopy, FTIR spectroscopy, XRD, EDS, SEM, TEM, AFM, DLS, and zeta-potential analysis according to standard nanoparticle characterization approaches (Mourdikoudis et al., 2018). The UV–visible spectrum was recorded over 300–700 nm. The supplied manuscript figures were retained for the characterization results.

2.4. Experimental animals and ethics

Healthy Wistar albino rats aged 6–8 weeks and weighing 180–220 g were obtained from an approved animal breeding facility. Animals were housed in polypropylene cages under standard laboratory conditions (25 ± 2 °C; 55–65% relative humidity; 12 h light/12 h dark cycle) with free access to standard pellet diet and water.

Animals were acclimatized for one week before experimentation. The experimental protocol was approved by the Institutional Animal Ethics Committee and reported as being conducted under CPCSEA registration No. 1824/PO/ERe/S/15/CPCSEA. The protocol was approved by the Institutional Animal Ethics Committee, with approval No. 42 dated 26 April 2026, Pinnacle Biomedical Research Institute, Bhopal, India.

2.5. Experimental design and stress induction

Animals were randomly allocated into four groups (n = 6 per group): Group I, normal control; Group II, stress-induced control; Group III, stress-induced animals treated with C. indica-mediated AuNPs (100 mg/kg body weight); and Group IV, stress-induced animals treated with carvedilol (20 mg/kg). Treatments were administered orally by gastric gavage approximately 1 h before the stress session. The reported stress paradigm combined restraint and foot-shock exposure: animals were restrained for 1 h, with mild electrical impulses reported as 0.2 mV applied through the grid floor at intervals of 15–20 min (Percie du Sert et al., 2020).

2.6. Biochemical evaluation

Blood samples were collected at the end of the experimental period and serum was separated by centrifugation. Urea, uric acid, creatine, and creatine phosphokinase were analyzed using standard biochemical procedures. Oxidative-stress markers, including SOD, CAT, GPx, GSH, and TBARS, were estimated using established methods (Aebi 1984; Marklund and Marklund 1974; Ohkawa et al., 1979).

2.7. Histopathological examination

Heart tissue was fixed in 10% formalin for 48 h and subsequently transferred to 70% alcohol. Tissues were processed, embedded in paraffin, sectioned at approximately 5 µm, stained with
hematoxylin and eosin, mounted in DPX, and examined microscopically. Photomicrographs were obtained using a Canon camera attached to a Carl Zeiss microscope (Suvarna et al., 2019).

2.8. Statistical analysis

Data were expressed as mean ± SD, consistent with the presentation of the supplied tables. Statistical analysis was performed using GraphPad Prism. Differences among experimental groups were analyzed by one-way analysis of variance (ANOVA) followed by Tukey's multiple-comparison test. A probability value of $p < 0.05$ was considered statistically significant.

3. Results

3.1. Preliminary phytochemical screening

Soxhlet extraction yielded a dark-brown semisolid methanolic extract with a reported yield of 15.24%. Qualitative screening indicated the presence of alkaloids, flavonoids, phenolic compounds, tannins, terpenoids, saponins, and steroids.

3.2. Visual confirmation of AuNP synthesis

Mixing the methanolic leaf extract with chloroauric acid produced a progressive colour change from pale yellow to ruby red. This visual change was consistent with subsequent spectroscopic and microscopic characterization of the nanoparticle preparation.

3.3. UV–visible spectroscopy

The nanoparticle suspension was scanned from 300 to 700 nm using a microplate reader (Epoch 2, BioTek). A maximum absorption band was observed at 525 nm, consistent with the surface plasmon resonance of colloidal AuNPs (Figure 1).

Figure 1. UV–visible absorption spectrum of C. indica-mediated AuNPs showing the surface plasmon resonance maximum at 525 nm.

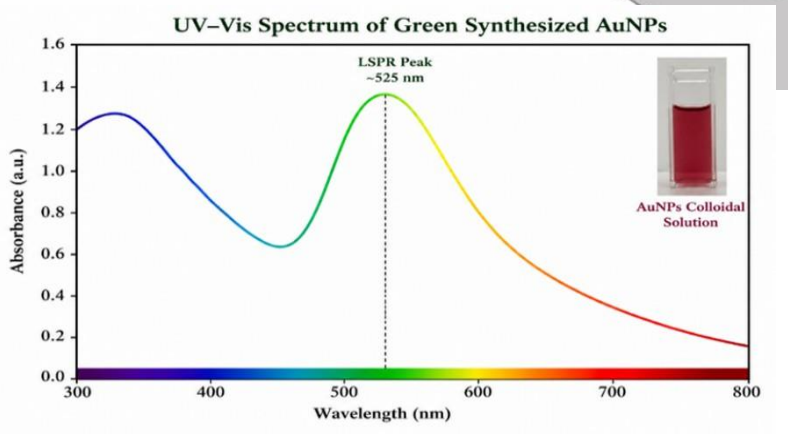

3.4. FTIR analysis

The FTIR spectrum displayed prominent bands at 3299.67, 1622.59, 1006.41, and 797.27 cm−1. These signals were assigned broadly to O–H/N–H stretching, carbonyl-associated vibrations, C–O groups, and lower-frequency surface-associated functional groups.

The pattern supports participation of plant-derived functional groups in nanoparticle formation and surface stabilization (Figure 2).

Figure 2. FTIR spectrum of C. indica-mediated AuNPs showing the principal absorption bands associated with surface functional groups.

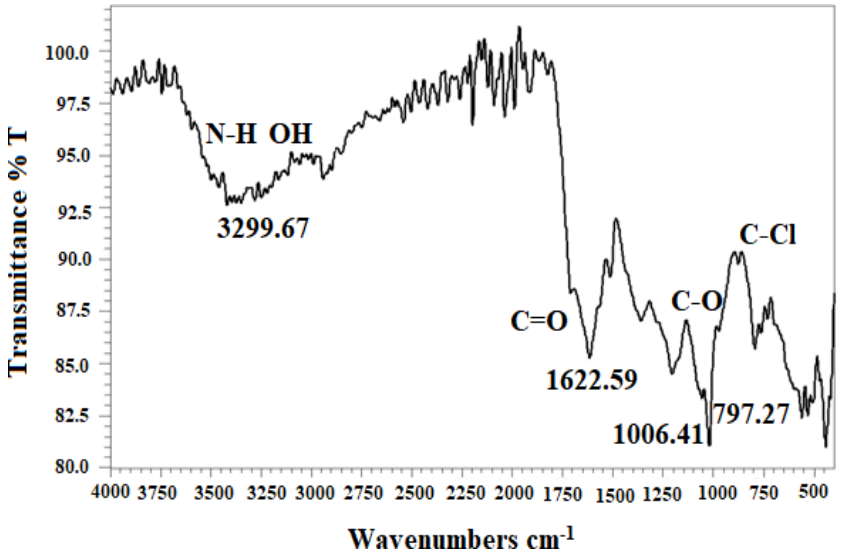

3.5. XRD analysis

The XRD pattern showed prominent reflections at 2θ = 38.14°, 44.76°, 64.80°, and 77.62°, corresponding to the (111), (200), (220), and (311) planes of face-centred cubic gold. These reflections are consistent with the characteristic diffraction pattern of metallic gold (JCPDS No. 04-0784) and support the crystalline nature of the synthesized AuNPs (Figure 3).

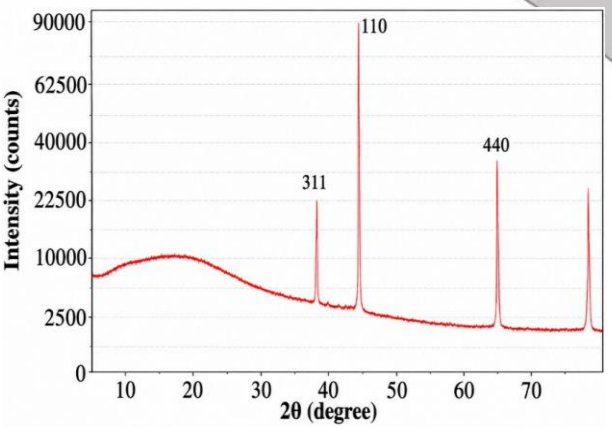

Figure 3. XRD pattern of C. indica-mediated AuNPs showing reflections corresponding to the (111), (200), (220), and (311) planes of face-centred cubic gold.

3.6. SEM analysis

SEM examination showed clustered nanoscale features. Six dimensions visible in the supplied micrograph were 46.65, 34.51, 31.52, 35.27, 38.74, and 34.62 nm, corresponding to a measured range of 31.52–46.65 nm (Figure 4).

Figure 4. SEM image of C. indica-mediated AuNPs showing measured nanoscale particle dimensions.

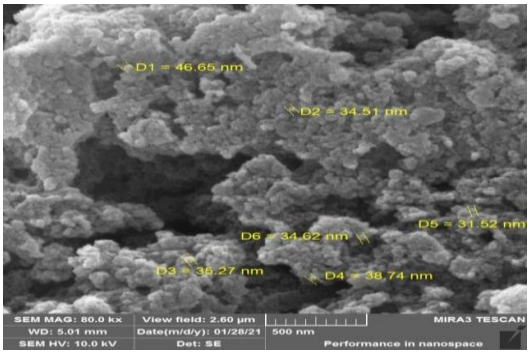

TEM, HRTEM, SAED and EDS

TEM images showed predominantly spherical nanoparticles with a mean particle diameter of 39.8 ± 0.8 nm. HRTEM showed an interplanar spacing of approximately 0.21 nm, compatible with the (200) lattice plane of face-centred cubic gold. SAED rings were indexed to the (111), (200), (220), and (311) planes, supporting the crystalline fcc structure. The supplied EDS figure reports Au, Cu, C, and O signals with values that differ between the displayed quantitative entries; therefore, the elemental composition is not quantitatively interpreted here (Figure 5).

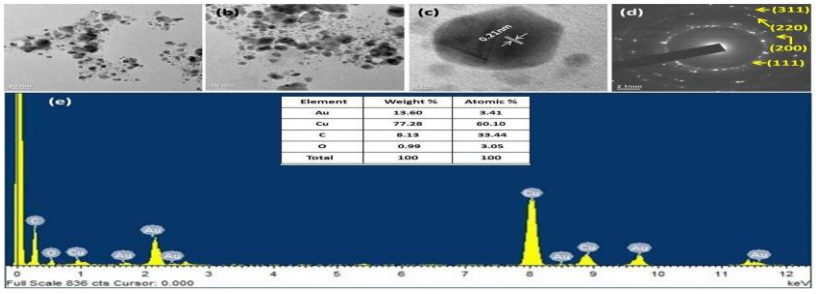

Figure 5. TEM and EDS characterization of C. indica-mediated AuNPs: (a,b) TEM images at different magnifications; (c) HRTEM image showing lattice fringes; (d) SAED pattern; (e) EDS spectrum/quantitative analysis

AFM topography

AFM imaging covered an area of approximately 1.2 × 1.2 µm. The supplied three-dimensional image indicates a vertical Z-range of approximately 39.8 nm and shows nanoscale surface topography. The three and two-dimensional AFM images are presented in Figures 6 and 7.

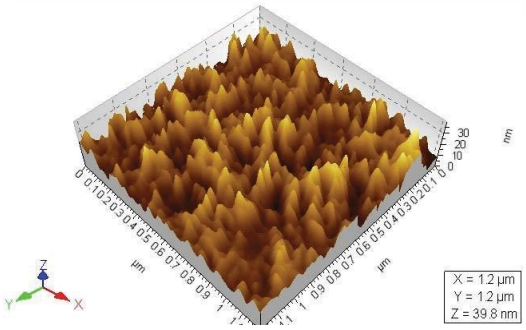

Figure 6. Three-dimensional AFM topography of C. indica-mediated AuNPs.

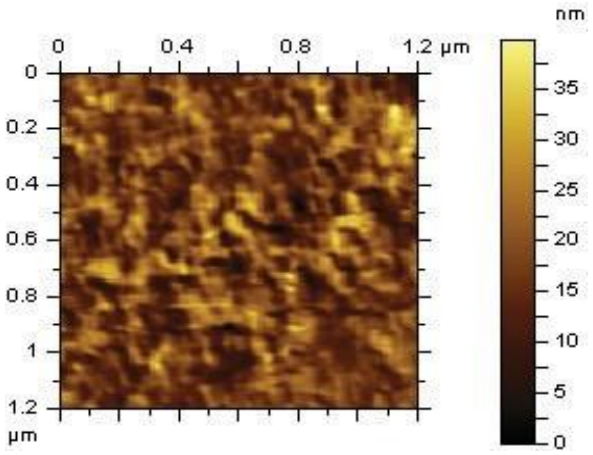

Figure 7. Two-dimensional AFM topography of C. indica-mediated AuNPs.

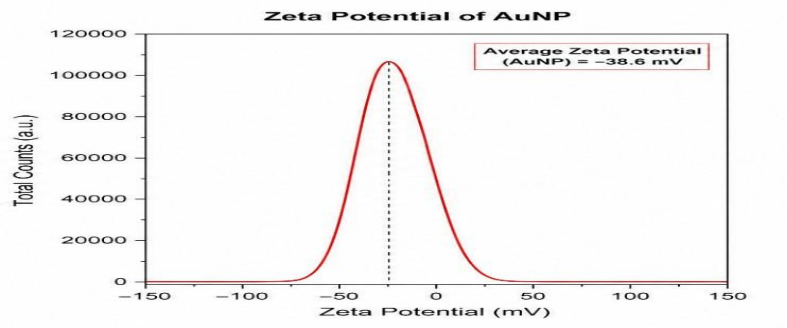

Figure 8. Zeta-potential profile of C. indica-mediated AuNPs showing an average potential of −38.6 mV.

Zeta potential

The AuNP preparation showed an average zeta potential of −38.6 mV. The negative surface charge is compatible with surface-associated anionic phytochemical groups and may contribute to colloidal stability (Figure 8).

Figure 8. Zeta-potential profile of C. indica-mediated AuNPs showing an average potential of −38.6 mV.

Protein level The stress-induced control showed a higher reported protein value than the normal control (Table 1).

Treatment with C. indica-mediated AuNPs reduced the value toward the normal-control level, while carvedilol produced an intermediate value. The reported group means were 12.55 ± 0.05, 26.50 ± 0.22, 12.45 ± 0.09, and 17.34 ± 0.18 mg/dL for Groups I–IV, respectively.

Table 1. Effect of C. indica-mediated AuNPs on protein level.

Group	Protein (mg/dL)
I. Normal	12.55 ± 0.05
II. Stress-induced control	26.50 ± 0.22
III. Stress-induced + AuNPs	12.45 ± 0.09
IV. Stress-induced + carvedilol	17.34 ± 0.18

Values are expressed as mean ± SD (n = 6). $p < 0.01$ for comparisons with the carvedilol-treated group.

Myocardial antioxidant enzymes

Stress exposure was associated with lower reported SOD, CAT, GPx, and GSH values than those observed in the normal-control group. AuNP treatment shifted these parameters toward the corresponding normal values, whereas carvedilol produced partial restoration (Table 2).

Table 2. Effect of C. indica-mediated AuNPs on myocardial antioxidant enzymes.

Group	SOD (IU/L)	CAT (IU/L)	GPx (IU/L)	GSH (IU/L)
I. Normal	34 ± 0.47	8.23 ± 0.27	57.3 ± 1.73	4.8 ± 0.73
II. Stress-induced control	19.3 ± 0.28	3.56 ± 0.28	27.5 ± 0.75	2.2 ± 0.15
III. Stress-induced + AuNPs	35 ± 0.23	8.2 ± 0.29	57.5 ± 1.38	4.8 ± 0.82
IV. Stress-induced + carvedilol	29 ± 0.45	5.2 ± 0.76	45 ± 1.98	4.1 ± 0.67

Values are expressed as mean ± SD (n = 6). $p < 0.01$ for comparisons with the carvedilol-treated group.

LDH and TBARS

Stress exposure increased LDH and TBARS concentrations. AuNP treatment reduced both parameters toward the normal-control values, while carvedilol produced a smaller reduction (Table 3). The reported LDH values were 91 ± 1.47, 203 ± 4.28, 92 ± 1.26, and 121 ± 1.03

IU/L, and TBARS values were 5.87 ± 0.05, 7.94 ± 0.22, 5.88 ± 0.36, and 6.27 ± 1.12 µmol/g tissue for Groups I–IV, respectively.

Table 3. Effect of C. indica-mediated AuNPs on LDH and TBARS levels.

Group	LDH (IU/L)	TBARS (µmol/g tissue)
I. Normal	91 ± 1.47	5.87 ± 0.05
Group	LDH (IU/L)	TBARS (µmol/g tissue)

II. Stress-induced control	203 ± 4.28	7.94 ± 0.22
III. Stress-induced + AuNPs	92 ± 1.26	5.88 ± 0.36
IV. Stress-induced + carvedilol	121 ± 1.03	6.27 ± 1.12

Values are expressed as mean ± SD (n = 6). $p < 0.01$ for comparisons with the carvedilol-treated group
Histopathology

The normal-control heart showed preserved myocardial architecture without evident tissue damage. The stress-induced control showed cytoplasmic vacuolation, disruption of myocardial fibres, intracellular edema, and widened interstitial spaces. The AuNP-treated group showed comparatively preserved myocardial architecture with less apparent edema and inflammatory change. The carvedilol-treated group also showed improvement relative to the stress-induced control (Figure 9).

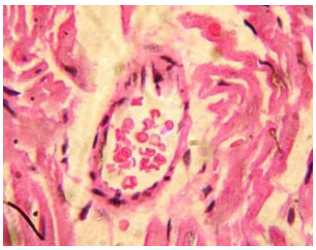

Normal control

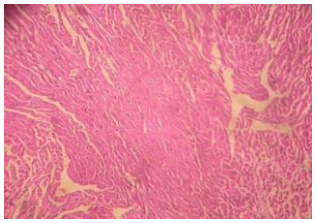

B. Stress-induced control

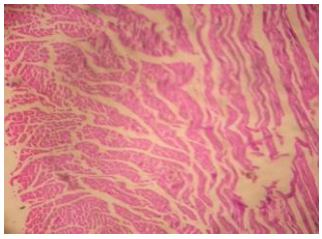

C. AuNP-treated

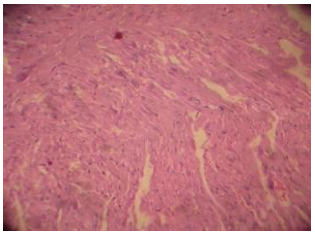

D. Carvedilol-treated

Figure 9. Histopathological sections of rat myocardium stained with hematoxylin and eosin: (A) normal control; (B) stress-induced control; (C) AuNP-treated group; (D) carvedilol-treated group. Original manuscript states 100× magnification.

4. Discussion

The present study demonstrates the feasibility of producing C. indica-mediated AuNPs and provides preliminary evidence of protective activity in a stress-induced myocardial injury model. The methanolic leaf extract contained several phytochemical classes, including phenolics and flavonoids that have previously been associated with antioxidant and metabolicactivities in C. grandis. Recent metabolomic profiling further supports the presence of diverse phenolic and flavonoid constituents in the leaves (Meenatchi et al. 2017; Lee et al., 2025). These compounds may contribute to the reducing and capping capacity of the plant extract during nanoparticle synthesis, although the present study did not chemically identify the individual capping molecules.

The colour transition to ruby red and the UV–visible absorption maximum at 525 nm provided initial evidence of AuNP formation. FTIR signals were consistent with plant-derived functional groups associated with the nanoparticle surface. XRD reflections at approximately 38°, 45°, 65°, and 78° were compatible with the characteristic fcc structure of metallic gold. SEM and TEM provided complementary information on particle dimensions, while the approximately 0.21-nm lattice spacing observed by HRTEM was compatible with the (200) plane. The negative zeta potential of −38.6 mV may contribute to colloidal stability. Collectively, these observations support successful formation of a crystalline AuNP preparation, although quantitative surface chemistry and long-term colloidal stability require additional analysis.

Stress-induced myocardial injury is linked to excessive sympathetic and HPA-axis activation, catecholamine exposure, oxidative imbalance, mitochondrial dysfunction, endothelial injury, and inflammatory signalling (Ghadri et al., 2018; Pelliccia et al., 2017). In the present model, stress was accompanied by lower antioxidant-enzyme values and higher LDH and TBARS values. The AuNP-treated group showed restoration of SOD, CAT, GPx, and GSH toward normal values together with reductions in LDH and TBARS. These biochemical changes were accompanied by improved myocardial histology. Because the study did not directly measure catecholamines, inflammatory mediators, mitochondrial function, or apoptotic signalling, the observed effects should be interpreted primarily as evidence of reduced oxidative and tissue injury rather than proof of a specific molecular mechanism.

The antioxidant response is biologically plausible because SOD converts superoxide radicals to hydrogen peroxide, while catalase and glutathione-dependent systems participate in subsequent detoxification and maintenance of redox balance (Birben et al., 2012). Phenolic and flavonoid constituents may also contribute to antioxidant activity, but the relative contribution of the plant-derived phytochemicals and the gold nanoparticle core cannot be separated in the current experimental design. A direct comparison with the carvedilol-treated group showed favourable biochemical and histological values for the AuNP preparation in this model; however, these preclinical findings do not establish superiority over carvedilol or predict clinical efficacy.

The study has several limitations. The sample size was small (n = 6 per group), the experiment used a single dose of the nanoparticle preparation, and mechanistic endpoints were limited. Detailed nanoparticle composition, batch-to-batch reproducibility, pharmacokinetics, tissue distribution, and systemic toxicity were not established. The EDS values should also be reconciled with the original instrument output before publication. Future studies should include dose-response experiments, appropriate nanoparticle and extract controls, validated molecular endpoints for oxidative stress and inflammation, cardiac functional measurements, pharmacokinetic studies, and comprehensive toxicological assessment. These steps are necessary to determine whether the observed cardioprotective signal is reproducible and mechanistically attributable to the C. indica-mediated AuNP formulation.

5. Conclusion

C. indica-mediated AuNPs were successfully prepared by a plant-assisted green synthesis approach and showed characteristic optical, structural, morphological, and surface-charge features of the synthesized nanoparticle preparation. In the experimental stress-induced myocardial injury model, AuNP treatment was associated with improved antioxidant parameters, lower LDH and TBARS values, and better preservation of myocardial architecture. The findings provide preliminary preclinical evidence supporting further investigation of this formulation as a potential experimental strategy for stress-associated myocardial injury. However, the results do not establish clinical efficacy or superiority over standard therapy. Additional studies addressing molecular mechanisms, dose optimization, pharmacokinetics, bio distribution, reproducibility, and toxicity are required before translational conclusions can be drawn.

6. Abbreviations

AFM, atomic force microscopy; ANOVA, analysis of variance; AuNPs, gold nanoparticles; CAT, catalase; DLS, dynamic light scattering; EDS, energy-dispersive X-ray spectroscopy; FTIR, Fourier-transform infrared spectroscopy; GPx, glutathione peroxidase; GSH, reduced glutathione; HAuCl4, chloroauric acid; HPA, hypothalamic–pituitary–adrenal; LDH, lactate dehydrogenase; ROS, reactive oxygen species; SEM, scanning electron microscopy; SOD, superoxide dismutase; TBARS, thiobarbituric acid reactive substances; TEM, transmission electron microscopy; XRD, X-ray diffraction.

7. References

1. Aebi H. 1984. Catalase in vitro. Methods in Enzymology 105: 121–126.Birben E, Sahiner UM, Sackesen C, Erzurum S, Kalayci O. 2012. Oxidative stress and antioxidant defense. World Allergy Organization Journal 5(1): 9–19.
2. Brotman DJ, Golden SH, Wittstein IS. 2007. The cardiovascular toll of stress. The Lancet 370(9592): 1089–1100.
3. Cohen S, Janicki-Deverts D, Miller GE. 2007. Psychological stress and disease. JAMA 298(14): 1685–1687.
4. Fatima Z, Saleem R, Khan RRM, Liaqat M, Pervaiz M, Saeed Z, et al. 2024. Green synthesis, properties, and biomedical potential of gold nanoparticles: A comprehensive review. Biocatalysis and Agricultural Biotechnology 59: 103271.
5. Ghadri JR, Wittstein IS, Prasad A, Sharkey S, Dote K, Akashi YJ, et al. 2018. International Expert Consensus Document on Takotsubo Syndrome (Part I): Clinical characteristics, diagnostic criteria, and pathophysiology. European Heart Journal 39(22): 2032–2046.
6. Harborne JB. 1998. Phytochemical Methods: A Guide to Modern Techniques of Plant Analysis. 3rd ed. Chapman & Hall, London.
7. Iravani S. 2011. Green synthesis of metal nanoparticles using plants. Green Chemistry 13: 2638–2650.
8. Kokate CK. 2008. Practical Pharmacognosy. Vallabh Prakashan, New Delhi.
9. Lee IY, Lee DH, Park JH, Joo N. 2025. UHPLC-HRMS/MS-based metabolic profiling and quantification of phytochemicals in different parts of Coccinia grandis (L.) Voigt. Food Science & Nutrition 13(2): e70004.
10. Meenatchi P, Purushothaman A, Maneemegalai S. 2017. Antioxidant, antiglycation and insulinotrophic properties of Coccinia grandis (L.) in vitro: Possible role in prevention of diabetic complications. Journal of Traditional and Complementary Medicine 7(1): 54–64.
11. Mehra V, Kumar S, Tamang AM, Chandraker SK. 2025. Green synthesis of gold nanoparticles (AuNPs) by using plant extract and their biological application: A review. BioNanoScience 15: 18.
12. Mourdikoudis S, Pallares RM, Thanh NTK. 2018. Characterization techniques for nanoparticles: Comparison and complementarity upon studying nanoparticle properties. Nanoscale 10: 12871–12934.
13. Ohkawa H, Ohishi N, Yagi K. 1979. Assay for lipid peroxides in animal tissues by thiobarbituric acid reaction. Analytical Biochemistry 95(2): 351–358.
14. Pelliccia F, Kaski JC, Crea F, Camici PG. 2017. Pathophysiology of Takotsubo syndrome. Circulation 135(24): 2426–2441.
15. Percie du Sert N, Hurst V, Ahluwalia A, et al. 2020. The ARRIVE guidelines 2.0: Updated guidelines for reporting animal research. BMJ Open Science 4(1): e100115.
16. Steptoe A, Kivimaki M. 2012. Stress and cardiovascular disease. Nature Reviews Cardiology 9: 360–370.
17. Suvarna KS, Layton C, Bancroft JD. 2019. Bancroft's Theory and Practice of Histological Techniques. 8th ed. Elsevier.